Polymer Chemistry

PAPER

Check for updates

Base-assisted degradable methacrylic polymer microcapsules synthesized *via* interfacial radical polymerization using 4,4-dimethyl-2-methylene-1,3-dioxolan-5-one (DMDL)

Tze Kwang Gerald Er, [iD] Wei Xiang Lim and Atsushi Goto [iD] *

Base-assisted degradable methacrylic polymer microcapsules were synthesized *via* interfacial radical polymerizations of oil-in-water emulsions containing 4,4-dimethyl-2-methylene-1,3-dioxolan-5-one (DMDL) as a monomer to provide degradable units in the obtained microcapsule shell. Many of the current degradable polymer microcapsules use ester linkages in the polymer backbones for degradation. The ester linkages incorporated into the polymer backbones can cause the polymers to be less stable, and the polymer microcapsules may gradually degrade hydrolytically under humidity. The DMDL units provide carbon–carbon linkages in the polymer backbones. The obtained microcapsules were stable under neutral aqueous conditions with various salts and selectively degraded under basic conditions. As a demonstration, a dye was encapsulated and was gradually released over time under basic aqueous conditions. Possible long-term storage stability under neutral aqueous conditions and selective content release under basic conditions may be advantages of the DMDL microcapsules.

1. Introduction

Polymeric microcapsules have attracted growing interest[1,2] and found applications in, *e.g.*, pharmaceutical delivery,[3–5] fabrication of self-healing materials,[6,7] and fragrance release.[8,9] Microcapsules are employed to encapsulate contents and protect them against environmental conditions, where the contents are physically separated from the surroundings by thin polymer shell layers. Microcapsules are also used for on-demand release of the contents by specific triggers such as pH, temperature, and enzymes.

Controlled release is attainable by incorporating degradable linkages in the polymer backbones in microcapsule shells.[10,11] Esters are often used as degradable linkages in the polymer backbones, which can be hydrolytically cleaved using pH[12–14] and enzymes.[14–16] Amide and carbonate linkages are also used for degradable linkages, although they are more difficult to degrade and often require additives to degrade. Thus, polyesters synthesized *via* polycondensation are typically used for degradable polymers. On the other hand, radical polymerization is usually not very suitable for introducing ester linkages into polymer backbones. A possible method is to use cyclic ketene acetal (CKA) monomers, and their radical ring opening polymerisation can afford ester linkages in the polymer backbones *via* ring opening of CKA monomers.[17–26] The incorporated ester linkages provide degradability. However, the ester groups incorporated into the polymer backbones can also cause the polymers to be less stable, and the polymer shells may gradually degrade hydrolytically under humidity and biologically *via* enzymes upon long-term storage.

Herein, we report the use of base-assisted (alkaline-assisted) degradation for content release. We synthesized degradable microcapsules using 4,4-dimethyl-2-methylene-1,3-dioxolan-5-one (DMDL) (Fig. 1) as a monomer that was previously reported by our group.[27,28] We conducted interfacial radical copolymerization of DMDL with other hydrophobic and hydro-
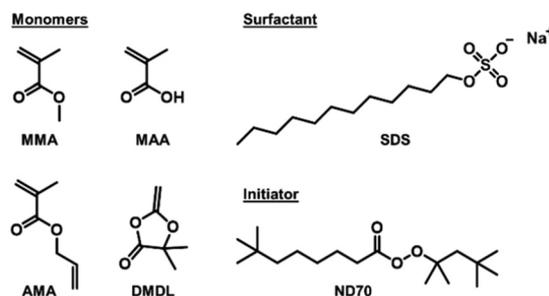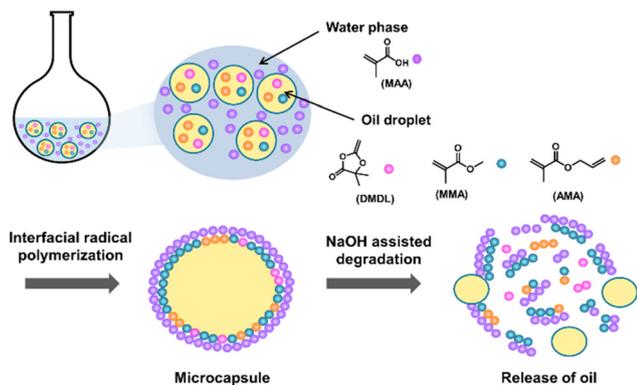
*School of Chemistry, Chemical Engineering and Biotechnology, Nanyang Technological University, 62 Nanyang Drive, 637459, Singapore.
E-mail: agoto@ntu.edu.sg*

Fig. 1 Chemical structures of the monomers, initiator, and surfactant used in this work.

Scheme 1 Synthesis of microcapsules *via* interfacial polymerization, subsequent degradation of microcapsules, and release of encapsulated contents.

philic methacrylic monomers (Fig. 1) to obtain microcapsules (Scheme 1). Interfacial polymerization is a useful technique to prepare microcapsules.[4,29–31] We prepared an oil-in-water emulsion. Oil droplets contained hydrophobic monomers and were dispersed in an aqueous continuous phase that contained a hydrophilic monomer. The polymer shell was formed at the interface (on the surface of the oil droplets). The DMDL units provide carbon–carbon linkages (not ester linkages) in the polymer backbones.[27,28] Because of the stable carbon–carbon linkages, the DMDL units in the polymer shells are stable under neutral aqueous conditions but can degrade only under basic conditions (Scheme 1). Thus, the DMDL microcapsules may be stored in a stable manner under neutral conditions and can selectively degrade under basic conditions, which can be an advantage of the DMDL microcapsules. The DMDL-containing microcapsules may find applications where content release under basic conditions is desirable, such as construction of self-healing materials,[32,33] pharmaceutical delivery,[12–14] scent release,[13] and pH sensing.[13] We studied the degradation of the obtained microcapsules under basic conditions and demonstrated the release of the encapsulated content using a fluorescent dye (Rhodamine B) as an example.

Fig. 1 shows the structures of the monomers, initiator, and surfactant used in this work.

2. Results and discussion

2.1. Interfacial polymerization

We conducted an interfacial radical polymerisation of MMA (30 equiv.) (hydrophobic monomer), DMDL (20 equiv.) (hydrophobic degradable monomer), AMA (10 equiv.) (hydrophobic crosslinkable monomer), and MAA (70 equiv.) (hydrophilic monomer) using chloroform (organic phase) and water (aqueous phase) as solvents (3/7 weight ratio), 1,1,3,3-tetramethylbutyl peroxyneodecanoate (ND70) (1 equiv.) as a hydrophobic radical initiator, and sodium dodecyl sulphate (SDS) as a surfactant. The total amount of the monomers was 30 wt%, the total amount of the solvents was 70 wt%, and the amount of the surfactant SDS was 0.1 wt% in the reaction mixture. The mixture was first mechanically stirred at 400 rpm at room temperature for 1 h to form an oil-in-water emulsion. The hydrophobic MMA, DMDL, and AMA monomers and the hydrophobic ND70 initiator would be mainly partitioned in the oil droplets, although they are not entirely hydrophobic and would be soluble in the aqueous phase to certain extents. The hydrophilic MAA monomer in its non-ionic carboxylic acid (COOH) form would be partitioned in both the aqueous phase and oil droplets. Then, the mixture was heated at 45 °C for 4 h with mechanical stirring at 800 rpm (Table 1, entry 1). Radicals were generated from the thermal initiator (ND-70) to initiate the polymerization and yield random copolymers consisting of hydrophobic monomer units and a certain number of MAA units inside the oil droplets. MAA would be continuously supplied from the aqueous phase to the oil droplets upon its consumption *via* the polymerization. The generated random copolymers were amphiphilic and tended to deposit at the interface between the oil and aqueous phases (on the surface of the oil droplets), forming microcapsules. We used the crosslinkable monomer AMA, which resulted in crosslinked polymeric shells to stabilize the microcapsules. We previously reported that the DMDL monomer may gradually

Table 1 Interfacial radical polymerization at 45 °C for 4 h

Entry	$[\text{MMA}]_0/[\text{DMDL}]_0/[\text{AMA}]_0/$ $[\text{MAA}]_0/[\text{ND70}]_0$ (molar ratio)[a,b]	Organic solvent	Organic solvent/ water (weight ratio)	Average diameter determined *via* SEM imaging[c] (μm)	Dv50[d] (μm)	Size distribution index[d]
1	30/20/10/70/1	CHCl$_3$	3/7	310	540	0.86
2	30/20/10/70/1	CHCl$_3$	4/6	No formation of capsules	NA	NA
3	30/20/10/70/1	CHCl$_3$	2/8	160	180	0.79
4	30/20/10/70/1	Chlorobenzene	2/8	260	380	0.84
5	30/20/10/70/1 (with Rhodamine B)	CHCl$_3$	2/8	110	140	0.70
C1	30/20/10/70/1 (without SDS)	CHCl$_3$	3/7	Aggregated capsules	NA	NA
C2	30/20/0/70/1	CHCl$_3$	3/7	Non-crosslinked capsules	NA	NA

[a] Stirring speed of 800 rpm. [b] 30 wt% of monomers (MMA, DMDL, AMA, and MAA) in total, 70 wt% of solvents (organic solvent and water) in total, and 0.1 wt% of SDS (no SDS for entry C1) in the entire mixture. [c] Determined using SEM in the dry state. [d] Determined using a particle size analyzer in water. Dv50 is a median particle size by volume (at the 50th percentile), and the size distribution index was determined as follows: size distribution index = (Dv90 − Dv10)/Dv50, where Dv90 and Dv10 are the particle sizes by volume at the 90th and 10th percentiles, respectively.

degrade in the presence of acids,[28] which could be a possible side reaction in the present system using MAA. However, in the present system, as mentioned, while DMDL would be preferentially partitioned in the oil phase, MAA would be gradually supplied from the aqueous phase to the oil phase upon its consumption, which would minimise the contact of the DMDL monomer with the acid (MAA) and hence minimize the degradation of the DMDL monomer. DMDL is less reactive than methacrylates (MMA, AMA, and MAA).[27] Thus, preferentially, methacrylate-rich amphiphilic random copolymers would be generated first, and DMDL-rich amphiphilic random copolymers would subsequently be generated. Then, at a late stage of polymerization, the pendant allyl group in the AMA unit and the residual DMDL (as well as the residual MMA, AMA, and MAA) would react to crosslink the polymeric shells. Because of the presence of the DMDL units in the crosslinking sites, the degradation of the DMDL units may effectively de-crosslink the polymeric shells (as described below). As a crosslinkable monomer, we chose AMA with a vinyl group and an allyl group instead of a monomer with two vinyl groups to delay the crosslinking, since the allyl group is less reactive than the vinyl group and would tend to remain until a late stage of polymerization.

The scanning electron microscopy (SEM) image (Fig. 2a) showed the formation of microcapsules with an average diameter of 310 μm in the dry state, which was calculated by taking an average of 30 capsules (10 capsules per image and across 3 images (Fig. S1 in the SI)). The microcapsules (Fig. 2a) had rough surfaces with indentations. These indentations might be ascribed to the volume contraction of the microcapsules by drying. When the shell was highly crosslinked, the rigid polymer shell might not be able to retain perfect spherical shapes but adjust the shell conformation to generate indentations. The formation of the indentations would support the successful synthesis of crosslinked microcapsules. We also determined the microcapsule size using a particle size analyzer in water (in the swollen state) (Table 1, entry 1). The median microcapsule size by volume (Dv50) (at the 50th percentile) was 540 μm in the swollen state, which is larger than that (310 μm) in the dry state because of the swelling.

Without the surfactant SDS (Table 1, entry C1), capsules were generated but aggregated, as observed with SEM (Fig. 2b). The result indicates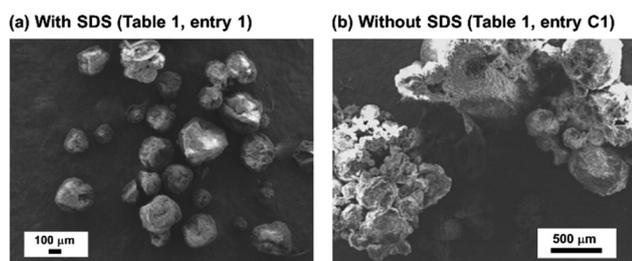 that agitation alone is insufficient for the synthesis of stable microcapsules and that the surfactant SDS is required.

With the surfactant SDS but without the crosslinkable AMA (Table 1, entry C2), we obtained non-crosslinked microcapsules. In contrast to the crosslinked microcapsule system (Table 1, entry 1), the polymer chains (as well as the remaining monomers) were soluble in solvents, *i.e.*, deuterated dimethyl sulfoxide (DMSO-d_6) for nuclear magnetic resonance (NMR) analysis and *N*,*N*-dimethylformamide (DMF) for gel permeation chromatography (GPC) analysis. Thus, we were able to determine the monomer conversions using ^{1}H NMR and characterize the primary (non-crosslinked) polymer structures using GPC and ^{1}H NMR. This non-crosslinked system may be viewed as a model system to monitor the polymerization behaviour and obtain information on the primary polymer structure, although the crosslinked and non-crosslinked systems may behave somewhat differently. Fig. 3a shows the plot of the overall monomer conversion *vs.* polymerization time. The overall monomer conversion reached 90% for 2 h and increased to 98% for 3 h and nearly 100% for 4 h. Thus, we conducted the polymerization for 4 h for all studied crosslinked systems, assuming virtually complete polymerizations for 4 h. Fig. 3b shows the plots of the number-average molecular weight (M_n) and dispersity ($Đ = M_w/M_n$) of the polymer *vs.* polymerization time, where M_w is the weight-average molecular weight. The carboxylic acids in the MAA units in the polymer were methylated using trimethylsilyldiazomethane to convert the MAA unit to the MMA unit to facilitate the GPC analysis (using tetrahydrofuran (THF) eluent). The M_n value was 13 500 g mol^{-1} at an early stage of polymerization for 20 min (4% monomer conversion) and gradually decreased to 5700 g mol^{-1} at a late stage of polymerization for 4 h (nearly 100% monomer conversion) because of the lower monomer concentration at a later stage of polymerization. The $Đ$ value was 3.43–4.66 during the polymerization. The pH value and zeta potential of the polymerization mixture were 2.3 and 290 mV at the start of the polymerization and 3.8 and 210 mV after the polymerization, respectively.
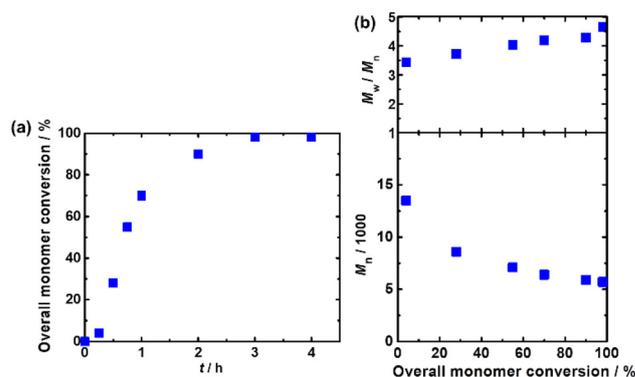

Fig. 2 SEM images of capsules synthesized (a) with SDS (Table 1, entry 1) and (b) without SDS (Table 1, entry C1).

Fig. 3 Plots of (a) overall monomer conversion *vs.* polymerization time and (b) M_n and M_w/M_n *vs.* overall monomer conversion for the non-crosslinked system using MMA (30 equiv.), DMDL (20 equiv.), MAA (70 equiv.), and ND70 (1 equiv.) (Table 1, entry C2).
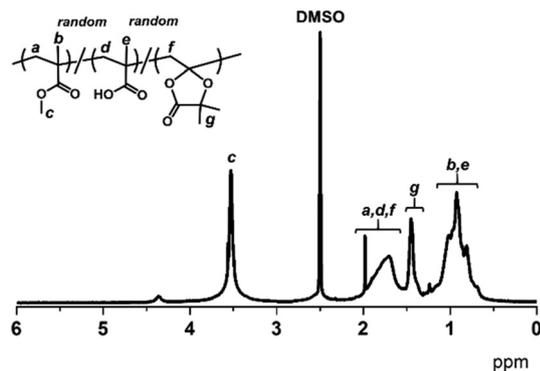
Fig. 4 ^{1}H NMR spectrum (DMSO-d_6) of the purified non-crosslinked polymer synthesized using MMA (30 equiv.), DMDL (20 equiv.), MAA (70 equiv.), and ND70 (1 equiv.) after 4 h of polymerization (Table 1, entry C2).

Fig. 4 shows the ^{1}H NMR spectrum of the polymer after 4 h of polymerization and purification (M_n = 6800 and $Đ$ = 4.30). For the purification, the polymerization mixture was acidified, dichloromethane was added, the organic phase was extracted, and the polymer was purified *via* reprecipitation in diethyl ether (non-solvent). The α-methyl (CH_3–C) protons of the MMA (proton *b*) and MAA (proton *e*) units appeared at 0.63–1.08 ppm, the side chain methyl (CH_3–O) protons of the MMA units (proton *c*) appeared at 3.31–3.76 ppm, and the side chain methyl (CH_3–C) protons of the DMDL units (proton *g*) appeared at 1.31–1.58 ppm. From the peak area ratios, we estimated the molar fractions of MMA, DMDL, and MAA in the polymer to be 27%, 14%, and 59%, respectively, which are consistent with those of the initial monomer molar (30/20/70) ratio (25%, 17%, and 58%, respectively).

2.2. Effects of the chloroform/water ratio and organic solvents

We varied the chloroform/water solvent weight ratio from 3/7 (Table 1, entry 1) to 4/6 and 2/8 (Table 1, entries 2 and 3). Stable capsules were not formed at the 4/6 ratio with more chloroform (Table 1, entry 2). The chloroform (oil) droplets

were fused and were not sufficiently stabilized by the utilized amount of surfactant SDS (0.1 wt%). Compared with the capsule (540 μm in the swollen state) at the 3/7 ratio, a smaller capsule (180 μm) was formed at the 2/8 ratio with less chloroform (Table 1, entry 3), because smaller oil droplets can be stabilized with the same amount of the surfactant.

Fig. 5a shows the SEM image of the capsules prepared at the 2/8 (chloroform/water) ratio (Table 1, entry 3), suggesting the formation of capsules. Fig. 5b shows the transmission electron microscopy (TEM) image of the capsules after mechanical rupture. Cavities were clearly observed, meaning that the obtained particles were true capsules (not fully occupied particles).

Instead of chloroform, we studied chlorobenzene as another organic solvent at the 2/8 (organic solvent/water) weight ratio (Table 1, entry 4, and Fig. 5c). The capsule size using chlorobenzene was 380 μm in the swollen state, which is larger than that (180 μm) using chloroform (Table 1, entry 3), because chlorobenzene ($\log P$ = 2.84) is more hydrophobic than chloroform ($\log P$ = 1.97) and the chlorobenzene droplets are more easily fused in water. Here, $\log P$ is a logarithm of a partition coefficient (P) of the molecule between 1-octanol and water phases (P = [moles of the molecule in 1-octanol]/[moles of the molecule in water]) and a larger $\log P$ value indicates greater hydrophobicity. The $\log P$ values in this work were estimated using the ChemDraw software.

2.3. Encapsulation and release of external content synthesis of biomass-based comb-shaped polyesters and their thermal properties

We encapsulated fluorescent dye (Rhodamine B) molecules in microcapsules and studied the degradation of the capsules and release of the content (Rhodamine B) molecules. We prepared the microcapsules under the mentioned conditions (Table 1, entry 3) using chloroform as an organic solvent at the 2/8 (chloroform/water) weight ratio, where Rhodamine B (0.25 wt% of the entire mixture) was added in the chloroform organic phase. Rhodamine B is a fluorescent molecule and was used as a visual indicator to show its encapsulation and release using a confocal microscope, as described below. We
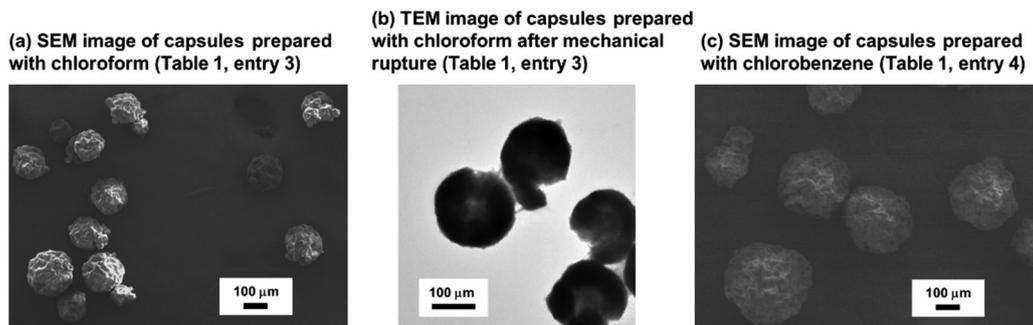

Fig. 5 (a) SEM image of capsules synthesized using chloroform as an organic solvent (Table 1, entry 3). (b) TEM image of capsules synthesized using chloroform as an organic solvent after rupture (Table 1, entry 3). (c) SEM image of capsules synthesized using chlorobenzene as an organic solvent (Table 1, entry 4).
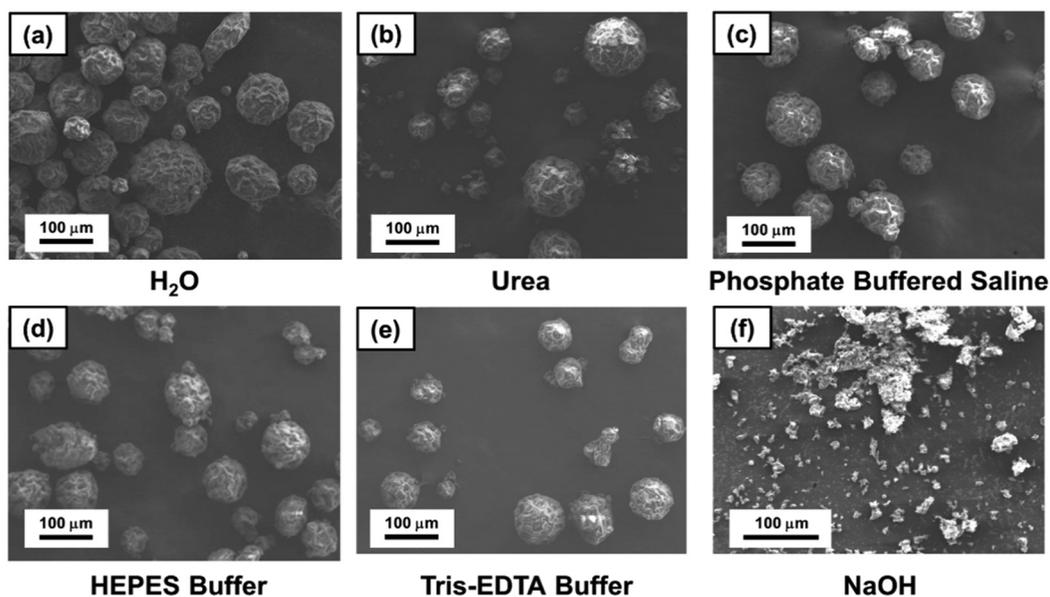
Fig. 6 SEM images of the Rhodamine B-encapsulated microcapsule (Table 1, entry 5) after immersing in (a) distilled water, (b) urea solution (10% urea in 90% water) (pH = 8.4), (c) phosphate buffered saline (pH = 7.4), (d) 4-(2-hydroxyethyl)-1-piperazineethanesulfonic acid (HEPES) buffer (pH = 7.3), (e) tris-ethylenediaminetetraacetic acid (tris-EDTA) buffer (pH = 7.5), and (f) sodium hydroxide (NaOH) solution (pH = 14) for 24 h.

obtained Rhodamine B-encapsulated microcapsules with 110 μm size in the dry state and 140 μm size in the swollen state (Table 1, entry 5), which have similar sizes to those (140 μm and 160 μm, respectively) of the microcapsules without Rhodamine B (Table 1, entry 3).

We first studied the stability of the obtained Rhodamine B-encapsulated microcapsule in six aqueous solutions. We dispersed 0.05 g of the dry capsule in 2 mL of aqueous solutions (2.5 wt% of the capsule) and stirred the dispersion at room temperature for 24 h. The microcapsule was stable in distilled water (Fig. 6a), urea solution (10% urea in 90% water) (pH = 8.4) (Fig. 6b), phosphate buffered saline (pH = 7.4) (Fig. 6c), 4-(2-hydroxyethyl)-1-piperazineethanesulfonic acid (HEPES)

buffer (pH = 7.3) (Fig. 6d), and tris-ethylenediaminetetraacetic acid (tris-EDTA) buffer (pH = 7.5) (Fig. 6e). On the other hand, the microcapsule degraded in a sodium hydroxide (NaOH) solution (pH = 14) (Fig. 6f). The result highlights that the DMDL-bearing capsule can selectively degrade under the basic conditions and can be retained in a stable manner under the neutral conditions with various salts. The degradation was also studied under weakly basic conditions at pH = 12 and 10. The microcapsules slightly degraded at pH = 12 for 24 h (Fig. S2a and S2b in the SI). The degradation at pH = 12 was slower than that at pH = 14 but still slightly occurred. At pH = 10, the microcapsules remained stable for the studied 24 h (Fig. S2c in the SI).
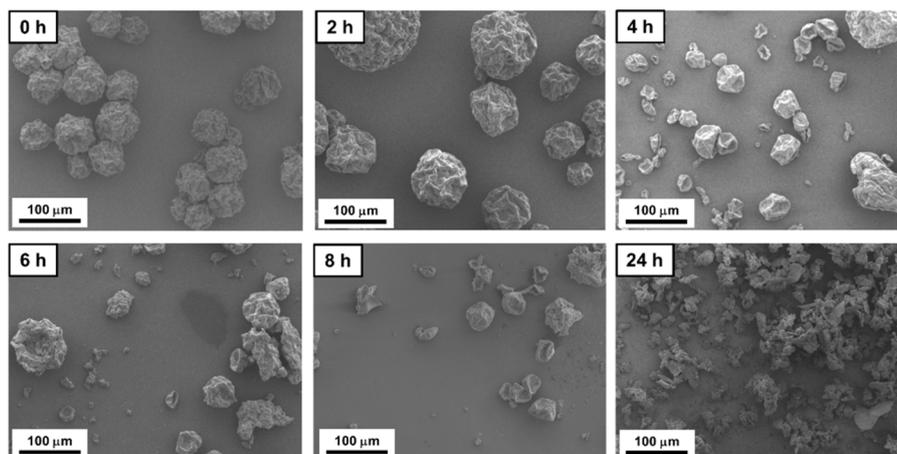

Fig. 7 SEM images of microcapsules at 0, 2, 4, 6, 8, and 24 h of degradation in an aqueous NaOH (pH = 14) solution.
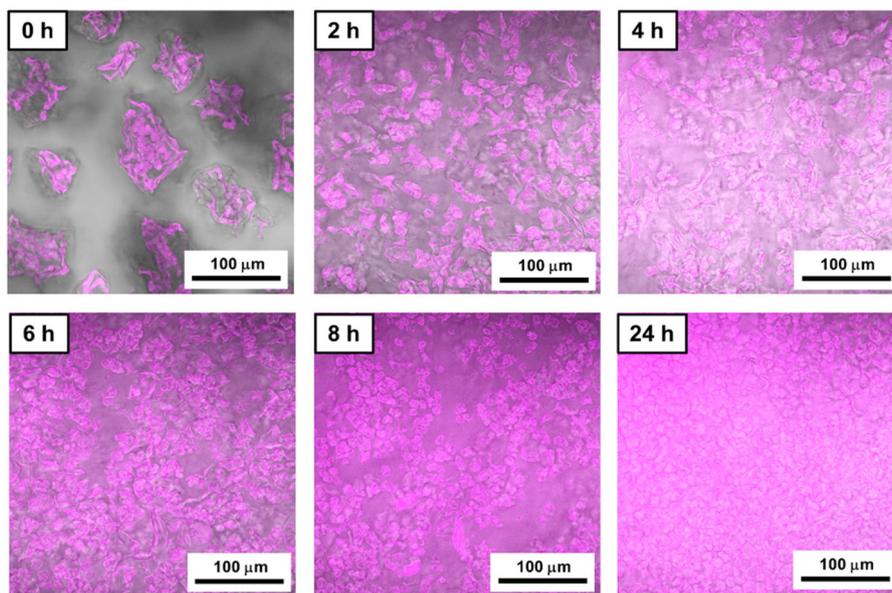
Fig. 8 Confocal microscopy images of Rhodamine B-loaded microcapsule dispersion (in the swollen state) at 0, 2, 4, 6, 8, and 24 h of degradation of the microcapsule in an aqueous NaOH (pH = 14) solution.

We studied the microcapsule degradation over time under basic conditions. We dispersed 0.05 g of the microcapsule in 5 mL of an aqueous NaOH solution (pH = 14) (1 wt% of the microcapsule) and stirred the dispersion at room temperature. Aliquots (0.5 mL) of the dispersion were taken out at time zero, 2 h, 4 h, 6 h, 8 h, and 24 h of stirring (degradation) and the microcapsule structures were studied using SEM. The SEM images in Fig. 7 show that the microcapsules gradually degraded over time, and only degraded fragments were observed after 24 h of degradation.

We also observed the release of Rhodamine B from the microcapsule over time using a confocal microscope. An aliquot (0.5 mL) of the degradation dispersion was neutralized using an aqueous hydrochloric acid (HCl) solution to pH = 6–7, and the resultant dispersion was observed in the swollen state using a confocal microscope (Fig. 8). We used an excitation wavelength of 514 nm and observed the emission of Rhodamine B at a wavelength of 580 nm. At time zero (before degradation), Rhodamine B was isolated in each microcapsule (Fig. 8). Rhodamine B started to diffuse from microcapsules after 2 h of degradation and further diffused from the microcapsules over time. After 24 h of degradation, Rhodamine B diffused into the entire mixture, indicating full release of Rhodamine B from the microcapsules. The result demonstrated gradual release of Rhodamine B over 24 h under the basic conditions.

3.   Conclusion

DMDL-containing microcapsules with 140–540 μm sizes (in the swollen state) were successfully synthesized through interfacial polymerizations using hydrophobic MMA, DMDL, and AMA and hydrophilic MAA. The DMDL units provided base-assisted degradability. The obtained microcapsules were stable

under neutral aqueous conditions with various salts, and they degraded under basic aqueous conditions. As a demonstration, a dye (Rhodamine B) was encapsulated and gradually released over time under basic aqueous conditions. Thus, the DMDL microcapsules may be stored under neutral conditions in a stable manner and can release the contents selectively under basic conditions in a controlled manner, which can be an advantage of the DMDL microcapsules.

Author contributions

Gerald Tze Kwang Er: writing – original draft, validation, investigation, formal analysis, data curation, and conceptualization. Lim Wei Xiang: validation, investigation, formal analysis, data curation, and conceptualization. Atsushi Goto: writing – original draft, validation, investigation, formal analysis, conceptualization, supervision, resources, project administration, and funding acquisition.

Conflicts of interest

The authors declare no competing financial interest.

Data availability

The data that support the findings of this study are available in the supplementary information (SI) of this article, including materials, synthesis, instrument, and SEM images. Supplementary information is available. See DOI: https://doi.org/10.1039/d5py01133g.

Acknowledgements

References

1 Q. Ke, Z. Qin, X. Yang, Q. Meng, X. Huang, X. Kou and Y. Zhang, *Carbohydr. Polym.*, 2025, **362**, 123699.

2 B. T. Lobel, D. Baiocco, M. Al-Sharabi, A. F. Routh, Z. Zhang and O. J. Cayre, *ACS Appl. Mater. Interfaces*, 2024, **16**, 40326–40355.

3 C. Yan and S. Y. Kim, *ACS Appl. Bio Mater.*, 2024, **7**, 692–710.

4 Y. Wang, N. Starvaggi and E. Pentzer, *Polym. Chem.*, 2023, **14**, 4033–4047.

5 D. Wei, Y. Sun, H. Zhu and Q. Fu, *ACS Nano*, 2023, **17**, 23223–23261.

6 T. Yimyai, D. Crespy and M. Rohwerder, *Adv. Mater.*, 2023, **35**, 2300101.

7 J. E. P. Christopher, M. T. H. Sultan, C. P. Selvan, S. Irulappasamy, F. Mustapha, A. A. Basri and S. N. A. Safri, *J. Mater. Res. Technol.*, 2020, **9**, 7370–7379.

8 M. Ng, S. El Habnouni and A. Goto, *ACS Appl. Polym. Mater.*, 2024, **6**, 9323–9334.

9 Z. Xiao, P. Sun, H. Liu, Q. Zhao, Y. Niu and D. Zhao, *J. Controlled Release*, 2022, **351**, 198–214.

10 S. Bag, D. Ghosh, S. Banerjee and P. De, *ACS Appl. Polym. Mater.*, 2025, **7**, 14033–14061.

11 S. A. Backer and L. Leal, *Acc. Chem. Res.*, 2022, **55**, 2011–2018.

12 J. F. Parente, V. I. Sousa, J. F. Marques, M. A. Forte and C. J. Tavares, *J. Controlled Release*, 2022, **2022**, 4640379.

13 L. Yang, Q. Yuan and J. Lin, *Text. Res. J.*, 2025, **95**, 2248–2272.

14 C. S. Dziewior, K. Godwin, N. G. Judge, N. Z. Dreger and M. L. Becker, *Prog. Polym. Sci.*, 2024, **156**, 101866.

15 C. T. Roberts and M. A. Grunlan, *ACS Macro Lett.*, 2025, **14**, 1221–1240.

16 M. S. Kim, H. C. Chang, L. Zheng, Q. Yan, B. F. Pfleger, J. Klier, K. Nelson, E. L. W. Majumder and G. W. Huber, *Chem. Rev.*, 2023, **494**, 153290.

17 A. Tardy, J. Nicolas, D. Gigmes, C. Lefay and Y. Guillaneuf, *Chem. Rev.*, 2017, **117**, 1319–1406.

18 T. Pesenti and J. Nicolas, *ACS Macro Lett.*, 2020, **9**, 1812–1835.

19 J.-B. Lena, A. W. Jackson, L. R. Chennamaneni, C. T. Wong, F. Lim, Y. Andriani, P. Thoniyot and A. M. van Herk, *Macromolecules*, 2020, **53**, 3994–4011.

20 A. W. Jackson, *Polym. Chem.*, 2020, **11**, 3525–3545.

21 A. Bossion, J. Chen, L. Guerassimoff, J. Mougin and J. Nicolas, *Nat. Commun.*, 2022, **13**, 2873.

22 C. Zhu and J. Nicolas, *Biomacromolecules*, 2022, **23**, 3043–3080.

23 Y. Deng, F. Mehner and J. Gaitzsch, *Macromol. Rapid Commun.*, 2023, **44**, 2200941.

24 C. Lefay and Y. Guillaneuf, *Prog. Polym. Sci.*, 2023, **147**, 101764.

25 F. Sbordone and H. Frisch, *Chem. – Eur. J.*, 2024, **30**, e202401547.

26 M. Ghorbani and E. Prince, *Biomacromolecules*, 2025, **26**, 118–139.

27 X. Y. Oh, Y. Ge and A. Goto, *Chem. Sci.*, 2021, **21**, 13546–13556.

28 T. K. G. Er, X. Y. H. Lim, X. Y. Oh and A. Goto, *Macromolecules*, 2024, **57**, 8983–8997.

29 S. Wang, Q. Zhang, J. Xiu, Y. Ma, L. Huang, L. Yi and H. Fu, *Micro Nano Lett.*, 2024, **19**, e70000.

30 C. Hu, H. Chen, J. Zheng, S. Zhou, X. Yang, K. Ngocho, T. Xie, K. Wang and J. Liu, *Adv. Funct. Mater.*, 2025, **35**, 2412408.

31 H. C. Cao, Y. Chen, Z. G. Qian, T. J. Huang, N. Zu, D. X. Zhang, W. Mu, B. X. Li and F. Liu, *Adv. Funct. Mater.*, 2025, **35**, 2412408.

32 S. Yu, J. Zhong, Y. Zhong, M. Yu, Z. Liu and L. Shen, *ACS Appl. Polym. Mater.*, 2024, **6**, 4005–4013.

33 P. Ghahremani, A. A. Sarabi and S. Roshan, *Surf. Coat. Technol.*, 2021, **427**, 127820.